THE JOURNAL OF PHYSICAL CHEMISTRY C
A JOURNAL OF THE AMERICAN CHEMICAL SOCIETY

pubs.acs.org/JPCC
Article

Synergistic p-Doping of Polymer-Wrapped Small-Diameter Single-Walled Carbon Nanotubes by Tris(pentafluorophenyl)borane

Sebastian Lindenthal, Daniel Rippel, Lucas Kistner, Angus Hawkey, and Jana Zaumseil*

Cite This: J. Phys. Chem. C 2025, 129, 5520−5529
Read Online

ACCESS | Metrics & More | Article Recommendations | Supporting Information

ABSTRACT: Despite its comparatively low electron affinity, tris(pentafluorophenyl)borane (BCF) has been widely explored as an efficient molecular p-dopant for semiconducting polymers through the formation of Brønsted acidic complexes as well as its high affinity toward Lewis-basic nitrogen moieties. Many conjugated polymers that are used for selective wrapping and dispersion of semiconducting single-walled carbon nanotubes (SWCNTs) such as poly[(9,9-di-*n*-octylfluorenyl-2,7-diyl)-*alt*-(6,6′-(2,2′-bipyridine))] (PFO-BPy) contain nitrogen moieties that should promote interaction with BCF. Here, we demonstrate that BCF indeed efficiently p-dopes even small-diameter (6,5) SWCNTs that are wrapped with large-bandgap PFO-BPy as corroborated by bleaching of the main absorption peaks and the appearance of red-shifted trion absorption and emission. In contrast, SWCNTs that are wrapped with poly(9,9-di-*n*-octylfluorenyl-2,7-diyl) (PFO) without any Lewis-basic nitrogen moieties are only mildly doped. UV−Vis−NIR absorption, ^{19}F NMR, and ^{11}B NMR spectra confirm that BCF dopes the bipyridine-containing PFO-BPy but not PFO, thus leading to a proposed doping mechanism that relies on the unique interactions between BCF, the bipyridine moieties in PFO-BPy, and the nanotubes. Since BCF doping of PFO-BPy-wrapped (6,5) SWCNTs is more efficient than doping with F_4TCNQ and more stable than doping with $AuCl_3$, it provides a reliable alternative for spectroscopic studies of the interactions of charge carriers and excitons in SWCNTs.

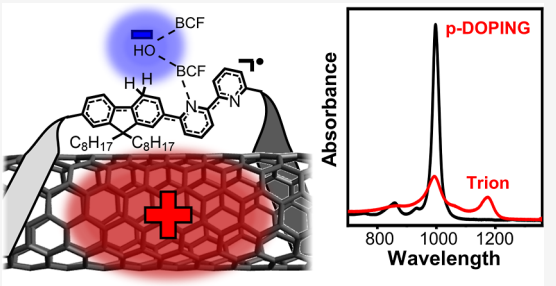

INTRODUCTION

Single-walled carbon nanotubes (SWCNTs) are quasi-one-dimensional carbon allotropes that can be conceptualized as seamlessly rolled-up sheets of graphene. Their structure is defined by two chiral indices (*n*,*m*), which directly determine their diameter as well as their electronic (metallic versus semiconducting)[1] and optical properties (absorption and emission wavelengths).[2] Since nanotube growth produces a mixture of different SWCNT species with different diameters, various methods to separate them such as selective dispersion by polymer-wrapping have been developed.[3−5] Polymer-wrapping of SWCNTs relies on specific interactions between the backbone of the conjugated polymers and the SWCNT lattice.[6] Hence, any changes to the electron density and structure of the polymer can also have a significant impact on the electronic and optical properties of the wrapped nanotubes.[7−9] The most selective and most commonly used wrapping polymers for small-diameter (<1 nm) nanotubes are the polyfluorene copolymers poly(9,9-di-*n*-octylfluorenyl-2,7-diyl) (PFO) and poly[(9,9-di-*n*-octylfluorenyl-2,7-diyl)-*alt*-(6,6′-(2,2′-bipyridine))] (PFO-BPy). They selectively wrap and thus disperse (7,5) and (6,5) nanotubes, respectively, in toluene (see Figure 1a).[3,10] They both have very large optical band gaps (>2.8 eV) and ionization energies (IEs), exceeding those of the respective nanotubes, which leads to the formation of type I heterojunctions.[8]

The control of charge carrier density in semiconducting polymers and SWCNTs through chemical doping is crucial for a wide range of applications, most recently for thermoelectric generators.[11,12] Doping also changes their optical properties by bleaching the ground state absorption and quenching photoluminescence accompanied by the appearance of charge induced absorption and emission (i.e., polaron or trion) bands.[13−15] These spectral changes can give direct insights into the interactions of charge carriers with electronic states or other quasiparticles (e.g., excitons), which strongly depend on the material. For the purpose of this study, we will only consider p-doping.

A variety of molecular dopants and different doping mechanisms have been studied for organic and polymeric semiconductors.[16] Molecular doping can be categorized as charge transfer doping, Brønsted acid doping, or Lewis acid doping. In the first case, the interaction of a molecular oxidant with an organic semiconductor leads to either full electron transfer—i.e., integer charge transfer (ICT) doping—or the

Received: December 19, 2024
Revised: February 20, 2025
Accepted: February 26, 2025
Published: March 5, 2025

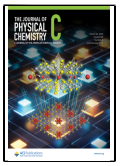

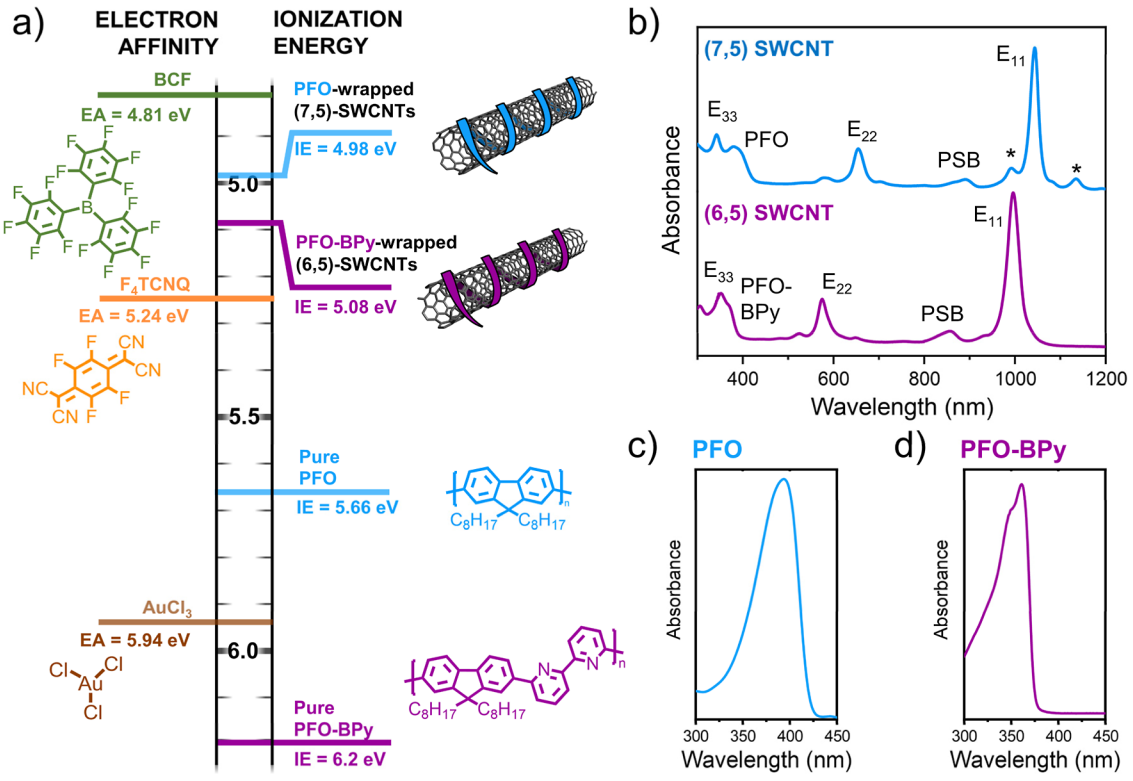

Figure 1. (a) Molecular structures of dopants and semiconductors used in this study and their corresponding EAs and IEs. EAs for dopants were retrieved from Han et al.,[33] Vijayakumar et al.,[39] and Lu et al.[40] IPs of SWCNTs were obtained from Tanaka et al.,[41] and IEs of polymers from Balcı Leinen et al. and Park et al.[8,42] (b) Absorption spectra of dispersions of PFO-wrapped (7,5) SWCNTs (top, blue) and PFO-BPy-wrapped (6,5) SWCNTs (bottom, purple) in toluene. Minority species of other semiconducting nanotubes in the (7,5) SWCNT dispersion are marked with an asterisk; PSB refers to the phonon sideband of the main excitonic E_{11} transition. (c,d) Absorption spectra of pure PFO and PFO-BPy in toluene, respectively.

formation of a charge transfer complex (CTC doping).[17,18] Common oxidants for charge transfer p-type doping of organic semiconductors and SWCNTs include $AuCl_3$, and F_4TCNQ (see Figure 1a). These dopants, however, often exhibit limited solubility in nonpolar solvents[19,20] or high chemical reactivity, which results in unwanted side reactions and limited doping stability.[21,22] Furthermore, effective p-doping by electron transfer generally occurs when the electron affinity (EA) of the dopant exceeds the IE of the semiconductor. For example, F_4TCNQ only induces weak doping in semiconductors with a relatively high IE, such as small-diameter carbon nanotubes.[14] Brønsted acids (e.g., hydrochloric acid and toluene sulfonic acid) are also effective dopants and have been applied extensively to polymers[23,24] and carbon nanotubes.[25,26] The mechanism of Brønsted acid doping is still unclear, but likely involves protonation of the organic semiconductor, followed by electron transfer between a charged and neutral semiconductor species or segment.[27]

While charge transfer doping and Brønsted acid doping have been utilized for organic semiconductors for decades, Lewis acid p-doping is a relatively new approach.[28] It involves the coordination of nonoxidative Lewis acids (e.g., AlX_3, BX_3, with X = F, Cl, Br) to Lewis basic moieties (e.g., pyridinic nitrogen), thus altering their electronic properties.[28,29] In particular, the strong Lewis acid tris(pentafluorophenyl)borane ($B(C_6F_5)_3$ or BCF, see Figure 1a) has been used recently to dope or co-dope organic semiconductors.[30] Its presence significantly enhanced the performance of organic light-emitting diodes,[31] field-effect transistors,[32,33] solar cells,[34,35] and thermoelectric devices.[36] Despite its comparatively low EA of only 4.81 eV, it can p-dope nitrogen-containing Lewis basic polymers with high ionization energies of up to 5.82 eV.[33] However, BCF can also dope polymers without Lewis basic moieties. This effect was recently attributed to the formation of strongly Brønsted acidic complexes of BCF with water ($BCF:OH_2$), which are capable of protonating polymer chains without Lewis basic moieties similar to other Brønsted acids.[37,38] However, these $BCF:OH_2$ complexes do not form in the presence of highly Lewis-basic moieties as BCF preferentially coordinates to them.[36−38]

Here, we employ BCF as a p-dopant for polymer-wrapped semiconducting carbon nanotubes with small diameters in toluene dispersions. We find that the doping efficiency, and hence impact on the optical properties of (6,5) and (7,5) nanotubes, depends on the presence of Lewis basic bipyridine units in the wrapping-polymer (PFO-BPy or PFO, respectively) and the concentration of the polymer when bipyridine units are present. We propose a possible doping mechanism based on ^{11}B NMR and ^{19}F NMR measurements. Compared with other common dopants for SWCNTs, BCF enables well-controlled, efficient, and stable p-doping of PFO-BPy-wrapped SWCNTs in toluene dispersions. It is thus an excellent choice for detailed spectroscopic studies of charge carriers in semiconducting nanotubes.

METHODS

Materials. All chemicals were used as purchased. Dopants were stored in a dry nitrogen glovebox, and doping solutions were freshly prepared on the day of usage. Doping experiments

https://doi.org/10.1021/acs.jpcc.4c08584
J. Phys. Chem. C 2025, 129, 5520−5529

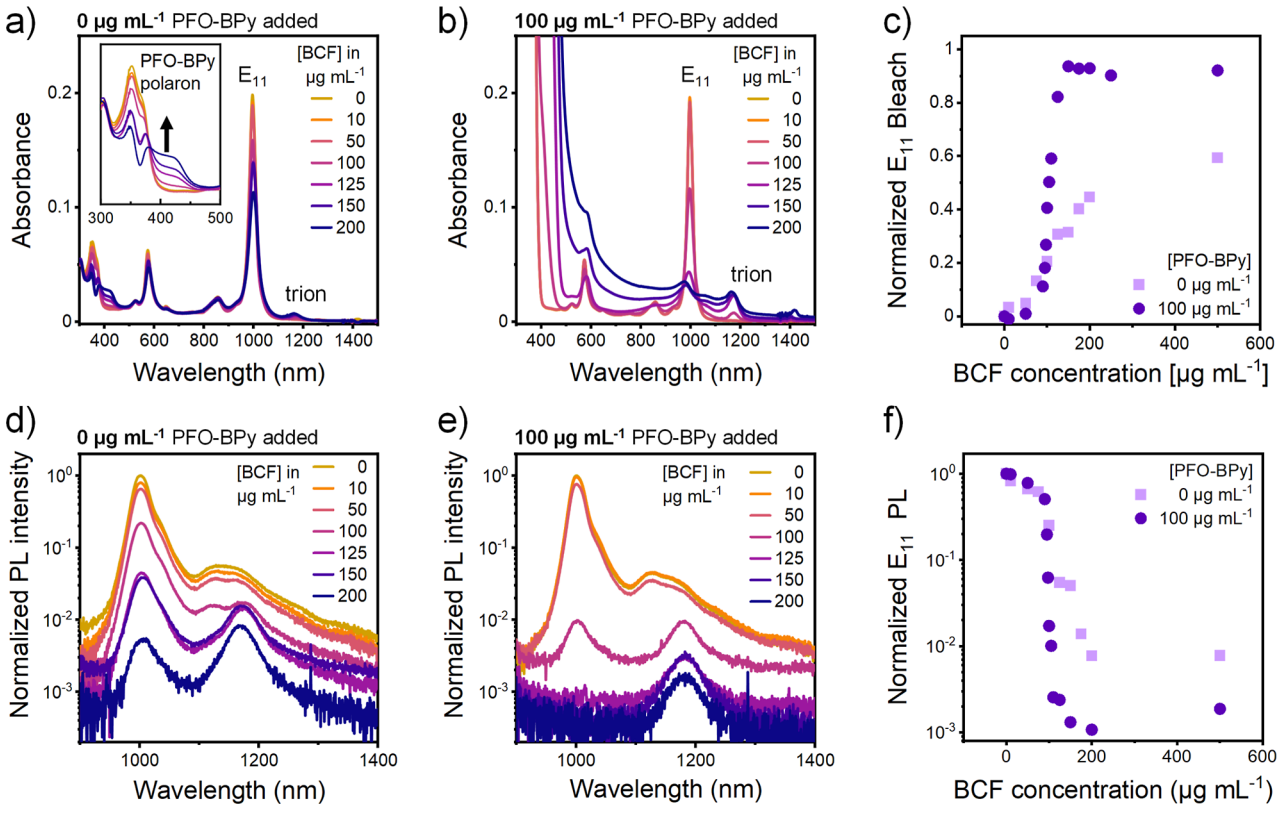

Figure 2. (a) Absorption spectra of PFO-BPy-wrapped (6,5) SWCNTs redispersed in pure toluene and doped with different concentrations of BCF, inset: PFO-BPy polaron absorption. (b) Absorption spectra of (6,5) SWCNTs, redispersed in a 100 μg mL^{-1} solution of PFO-BPy in toluene, doped with different amounts of BCF. (c) E_{11} absorption bleach values, extracted from extended data shown in Figure S4. (d) Normalized PL spectra of (6,5) SWCNTs redispersed in pure toluene and doped with different amounts of BCF. (e) Normalized PL spectra of (6,5) SWCNTs, redispersed in a 100 μg mL^{-1} solution of PFO-BPy in toluene and doped with different amounts of BCF. (f) Normalized E_{11} PL intensity plotted against the BCF concentration.

were performed under atmospheric conditions and with non-dried solvents. $AuCl_3$ (≥99.99%) and 2,3,5,6-tetrafluoro-7,7,8,8-tetracyanoquinodimethane (>97%) were purchased from Sigma-Aldrich. Tris(pentafluorophenyl)borane (>98%) was purchased from Tokyo Chemical Industries (TCI) and 2,2′-bipyridine (>99.94%) was acquired from BLD Pharmatech.

Selective Dispersion of SWCNTs. Dispersions of (6,5) SWCNTs or (7,5) SWCNTs were produced by shear force mixing (Silverson L2/Air, 10,230 rpm, 20 °C, at least 72 h) of CoMoCAT raw material (Sigma-Aldrich, SG65i, 0.5 g L^{-1}) in a solution of poly[(9,9-dioctylfluorenyl-2,7-diyl)-*alt*-(6,6′-(2,2′-bipyridine))] (PFO-BPy, American Dye Source, M_W ∼ 38 kDa, 0.5 g L^{-1}) or poly(9,9-dioctylfluorenyl-2,7-diyl) (PFO, Sigma-Aldrich, M_W > 20 kDa, 0.9 g L^{-1}) in toluene. The resulting slurry was centrifuged twice at 60,000*g* for 45 min (Beckman Coulter Avanti J26SXP centrifuge). Finally, the supernatant was filtered through a poly(tetrafluoroethylene) (PTFE) syringe filter (Whatman, pore size of 5 μm). Further details can be found in Graf et al. and Lindenthal et al.[43,44]

Controlling the Polymer Concentration in SWCNT Dispersions. (6,5) or (7,5) SWCNT-dispersions were filtered through a poly(tetrafluorethylene) (PTFE) membrane filter (Merck Omnipore, JVWP, pore size 0.1 μm). The resulting filter cakes were submerged in hot toluene (80 °C, 8 times for 10 min) to wash away residual free polymer. Small parts of the filter cake were sonicated (Branson 2510, 30 min at 20 °C) in either pure toluene or a solution of the respective wrapping polymer in toluene to yield SWCNT dispersions with a controlled polymer concentration.

Doping of Polymers. Stock solutions of PFO and PFO-BPy were created by dissolving 1 mg mL^{-1} of the respective polymer in either toluene (for absorption measurements) or d^8-toluene (for NMR measurements). Stock solutions of the polymers were then mixed with (d^8-)toluene and a freshly prepared stock solution of BCF (1 mg mL^{-1}) in (d^8-)toluene to achieve the desired doping levels.

BCF and F_4TCNQ Doping Procedure. Stock solutions of either BCF (1 mg mL^{-1}) or F_4TCNQ (0.5 mg mL^{-1}) and wrapping polymer (PFO or PFO-BPy, 1 mg mL^{-1}) in toluene were mixed with freshly sonicated SWCNT dispersions and pure toluene, such that the resulting samples contained a SWCNT concentration corresponding to an optical density of 0.2 cm^{-1} at the E_{11} transition and the desired concentrations of wrapping polymer and BCF. Absorption and photoluminescence (PL) spectra were recorded within 15 min of preparing each sample to minimize effects of dedoping or doping-induced aggregation.

$AuCl_3$ Doping Procedure. Stock solutions of $AuCl_3$ (0.5 mg mL^{-1}) and wrapping polymer (1 mg mL^{-1}) in a volumetric 5:1 mixture toluene/acetonitrile were combined with SWCNT dispersions and pure toluene and acetonitrile. The resulting samples contained a SWCNT concentration corresponding to an optical density of 0.2 cm^{-1} at the E_{11} transition, the desired concentrations of wrapping polymer and $AuCl_3$, while maintaining a volumetric ratio of 5:1 toluene/acetonitrile.

https://doi.org/10.1021/acs.jpcc.4c08584
J. Phys. Chem. C 2025, 129, 5520−5529

NMR Spectroscopy. NMR spectra were recorded with a Bruker Avance III 600 (field intensity of 14.1 T, ^{1}H: 600.18 MHz) with d^{8}-toluene as the solvent. Chemical shifts (δ) are reported in parts per million in relation to $CFCl_3$ for ^{19}F NMR spectra and BF_3−Et_2O for ^{11}B NMR spectra. Note that no standard was used to avoid possible interactions with BCF. Analysis of the spectra was performed with MestReNova x64. The molar ratios of PFO-BPy/BCF mixtures are expressed as the ratio of polymer monomer units/BCF. Since the molar weights of PFO-BPy monomers and BCF are quite similar, the molar ratio roughly resembles the mass ratio of BCF/PFO-BPy.

Absorption Spectroscopy. Absorption spectra were recorded with a Cary 6000i UV−vis−NIR absorption spectrometer (Varian, Inc.) and quartz cuvettes with either a 0.1 or 1 cm path length. For SWCNTs, the resulting spectra were fitted with the Fityk 1.3.1 software by subtracting a Naumov background and fitting the peaks with Gaussian line profiles to obtain absorbances (A) for the E_{11} absorbance peaks; for details see Pfohl et al.[45] The normalized bleach was calculated as $1 - A(E_{11})/A(E_{11})_{reference}$.

Photoluminescence Spectroscopy. PL spectra were acquired from (6,5) SWCNT dispersions by excitation at 575 nm with a picosecond-pulsed supercontinuum laser (NKT) Photonics SuperK Extreme. Emitted photons were collected by a NIR-optimized 50× objective (N.A. 0.65, Olympus) and spectra were recorded with an Acton SpectraPro SP2358 spectrometer with a liquid-nitrogen-cooled InGaAs line camera (Princeton Instruments, OMA-V:1024). A lamp spectrum of a stabilized tungsten halogen lamp (Thorlabs SLS201/M, 300−2600 nm) was recorded at regular intervals to perform detection efficiency corrections.

RESULTS AND DISCUSSION

Doping of PFO-BPy-Wrapped (6,5) SWCNTs with BCF. Dispersions of PFO-BPy-wrapped (6,5) SWCNTs and PFO-wrapped (7,5) SWCNTs in toluene were obtained via shear-force mixing (for details, see Methods). Figure 1b shows the corresponding absorption spectra with their characteristic E_{11} and E_{22} absorption peaks for the sorted nanotube species and a few minority species that were present. Raman spectra, recorded on drop-cast films of SWCNTs (Figure S1), indicated small amounts of other semiconducting SWCNTs but no metallic nanotubes. Arnold and co-workers had shown previously that the coverage of different nanotube species with polyfluorene wrapping polymer depends strongly on the concentration of the latter in solution.[46] Hence, we controlled the concentration of the polymer (PFO-BPy or PFO) for all doping experiments (see Methods) by removal of excess polymer from the initially obtained dispersions via filtration and subsequent dispersion in pure toluene (0 μg mL^{-1}) or in a polymer solution (100 μg mL^{-1}) to adjust its concentration (see Figure S2a−c). Note that it is not possible to remove all of the wrapping polymer, hence the diluted dispersions as used for doping studies still contained about 1 μg mL^{-1} PFO-BPy (see Figure S2d), which should lead to submonolayer coverage of the SWCNTs (around 50%).[46] The same applies to (7,5) SWCNTs dispersions with PFO (Figure S3).

Doping experiments with BCF were performed at an absorbance of 0.2 at the E_{11} transition of the SWCNTs (corresponding to ∼0.36 μg mL^{-1} of SWCNTs) and a constant PFO-BPy concentration of either 0 or 100 μg mL^{-1}. At a polymer concentration of 100 μg mL^{-1} (PFO-BPy/SWCNTs ≈ 280:1), we expect full coverage of the SWCNTs by PFO-BPy.[46] All dispersions were sonicated prior to each doping experiment to minimize the influence of aggregation. Absorption spectra of BCF-doped (6,5) SWCNTs with and without added PFO-BPy are shown in Figure 2a,b. Upon addition of increasing amounts of BCF, the (6,5) SWCNT E_{11} transition is bleached and a red-shifted absorption between 1160 and 1180 nm appears, which is ascribed to a trion (charged exciton).[14] These spectral changes are typical for p-doping of SWCNTs and have been reported for several different dopants.[47−49]

The evolution of the normalized bleach of the E_{11} absorption with increasing BCF concentration for (6,5) SWCNTs without additional PFO-BPy is shown in Figure 2c. For BCF concentrations of less than 100 μg mL^{-1} only a slight bleach (∼15%) can be observed. At BCF concentrations above 100 μg mL^{-1} the SWCNTs are increasingly doped and E_{11} bleaching reaches ∼60% for the highest BCF concentration of 500 μg mL^{-1}. This behavior is similar to chemical doping with common oxidants such as F_4TCNQ and $AuCl_3$.[50]

For low PFO-BPy concentrations (Figure 2a), it is also possible to follow the doping process of the residual PFO-BPy in the (6,5) SWCNT dispersion (see Figure S4 for a complete set of spectra with BCF concentrations up to 500 μg mL^{-1}). Interestingly, the PFO-BPy polaron at 420 nm (for spectra of BCF-doped PFO-BPy without SWCNTs see Figure S5a) emerges at exactly the same BCF concentration as the SWCNT trion (i.e., at 100 μg mL^{-1}). The PFO-BPy polaron, the E_{11} bleach and the SWCNTs trion absorption all follow the same trend as a function of the BCF concentration (Figure S6). This is not the case for other dopants (e.g., $AuCl_3$), which strongly dope (6,5) SWCNTs but not the wrapping polymer[48] and indicates a synergistic interaction between BCF, PFO-BPy and the SWCNTs.

Since a higher PFO-BPy concentration should result in higher polymer coverage of the SWCNTs,[46] we also expect a stronger BCF doping effect for (6,5) SWCNT dispersions doped at a PFO-BPy concentration of 100 μg mL^{-1}. Absorption spectra of these dispersions (Figure 2b) exhibit the same general trends for increasing BCF concentrations and indeed a significantly stronger doping at the same BCF concentrations. Up to a BCF concentration of 90 μg mL^{-1}, no bleaching occurs at all; however, between 90 and 110 μg mL^{-1} of BCF, the E_{11} bleach reaches more than 80% (Figure 2c). At even higher BCF concentrations, the E_{11} absorption peak nearly vanishes and the normalized bleach reaches ∼95%. These values are significantly higher than those for the (6,5) SWCNT dispersion without extra PFO-BPy.

Figure S7 gives a more detailed representation of the data in Figure 2c together with the corresponding absorption spectra. They show a strong blueshift (up to 20 nm) of the E_{11} absorption as previously discussed by Eckstein et al.[15] The peak position of the PFO-BPy polaron shifts from roughly 420 to 450 nm (Figure S8), thus indicating a higher doping level of the polymer. Again, the PFO-BPy polaron absorption, the SWCNT E_{11} bleach, and the SWCNT trion absorption for different BCF concentrations (Figure S9) follow the same trend, similar to the 0 μg mL^{-1} PFO-BPy sample (Figure S6).

As photoluminescence (PL) of SWCNTs is even more sensitive toward doping than absorption, we also recorded PL spectra of BCF-doped (6,5) SWCNT samples with and without added PFO-BPy (Figure 2d,e). For better comparability, the spectra were normalized to the E_{11} emission of the

https://doi.org/10.1021/acs.jpcc.4c08584
J. Phys. Chem. C 2025, 129, 5520−5529

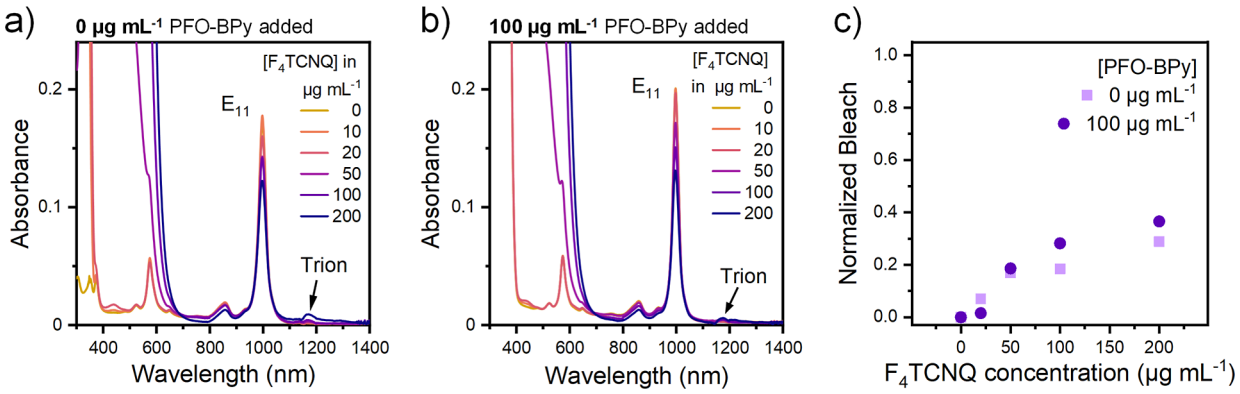

Figure 3. (a) Absorption spectra of (6,5) SWCNTs redispersed in pure toluene and doped with different amounts of F_4TCNQ. (b) Absorption spectra of (6,5) SWCNTs redispersed in a 100 μg mL^{-1} solution of PFO-BPy in toluene and doped with different amounts of F_4TCNQ. (c) Normalized E_{11} bleach values for both dispersions depending on the F_4TCNQ concentration.

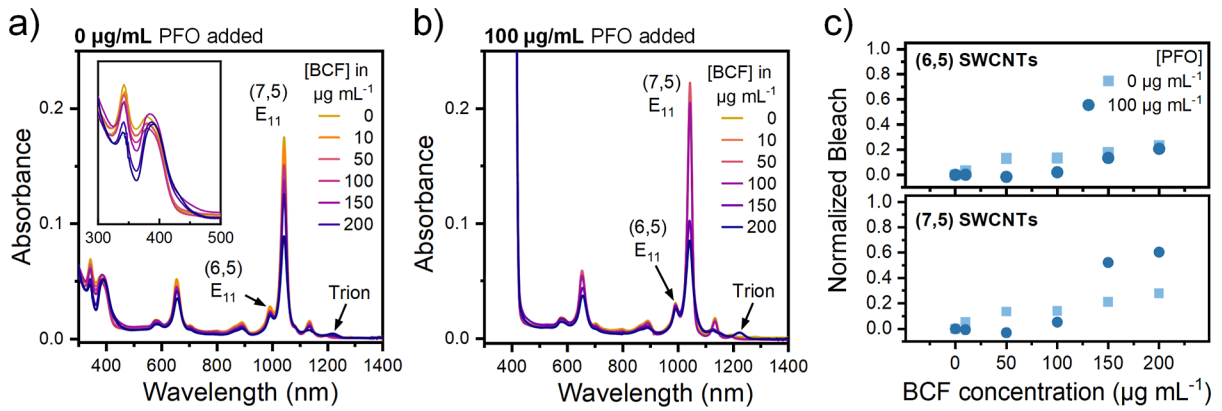

Figure 4. (a) Absorption spectra of PFO-wrapped (7,5) SWCNTs (with residual (6,5) SWCNTs) redispersed in pure toluene and doped with different amounts of BCF. (b) Absorption spectra of (7,5) SWCNTs redispersed in a 100 μg mL^{-1} solution of PFO in toluene and doped with different amounts of BCF. (c) Normalized E_{11} bleach values for PFO-wrapped (6,5) and (7,5) SWCNTs.

undoped sample, and the PL intensities were plotted on a logarithmic scale. Both types of samples showed very strong quenching of the E_{11} emission upon addition of BCF. Trion emission (at 1180 nm) also appeared as expected from previous reports on doped (6,5) SWCNTs.[50] Again, a clear difference in the degree of doping can be observed. While E_{11} emission remained visible for the 0 μg mL^{-1} PFO-BPy sample when doped with 200 μg mL^{-1} BCF, it was completely quenched in the 100 μg mL^{-1} PFO-BPy sample. Plotting the normalized E_{11} emission for both experiments against the BCF concentration (Figure 2f) further shows that a higher PFO-BPy concentration leads to overall stronger quenching compared to samples without additional PFO-BPy.

This significantly stronger doping of the (6,5) SWCNTs by BCF when additional PFO-BPy is present and the simultaneous and similar doping trends of the wrapping polymer strongly indicate a synergistic effect between BCF and PFO-BPy with its bipyridine units in the doping process of the SWCNTs. However, the possibility of simultaneous but nevertheless independent doping of PFO-BPy and (6,5) SWCNTs cannot be excluded yet.

The observed doping of PFO-BPy wrapped (6,5) SWCNTs with BCF can be compared to the well-known molecular p-dopant F_4TCNQ at the same polymer concentrations. Corresponding absorption spectra and normalized bleaching values at different F_4TCNQ concentrations are presented in Figure 3a–c. The E_{11} bleach and trion absorption that are associated with increasing p-doping levels are observed again. The normalized bleach values of samples with 0 and 100 μg mL^{-1} PFO-BPy are very similar to each other and correspond to the levels obtained by BCF for 0 μg mL^{-1} PFO-BPy (see Figure 2a). Due to the strong absorption of F_4TCNQ in the same range as the PFO-BPy, a direct comparison between doping of the wrapping polymer and SWCNTs is not possible. Overall, there seems to be no specific interaction between PFO-BPy and molecular dopants in general, but the interaction between BCF and PFO-BPy appears to be crucial.

Doping of PFO-Wrapped (7,5) SWCNTs with BCF. To corroborate that PFO-BPy and its bipyridine unit indeed play an integral role in the BCF-doping of nanotubes, we tested the doping of PFO-wrapped (7,5) SWCNTs with BCF at PFO concentrations of 0 and 100 μg mL^{-1}. Due to the slightly smaller bandgap and lower ionization energy of the (7,5) SWCNTs compared to (6,5) SWCNTs (Figure 1a), we would expect even stronger doping of the (7,5) SWCNTs by BCF if solely Brønsted acid doping took place. Additionally, PFO does not wrap (7,5) SWCNTs as tightly as PFO-BPy wraps (6,5) SWCNTs,[51] which would facilitate access of a BCF:OH_2 complex[37,38] to the nanotube surface.

PFO is less selective toward (7,5) SWCNTs than PFO-BPy is toward (6,5) SWCNTs. Hence, depending on the polymer concentration, other semiconducting nanotube species such as (6,5) SWCNTs will also be dispersed by PFO from the CoMoCat nanotube source material. This is evident from the

https://doi.org/10.1021/acs.jpcc.4c08584
J. Phys. Chem. C 2025, 129, 5520−5529

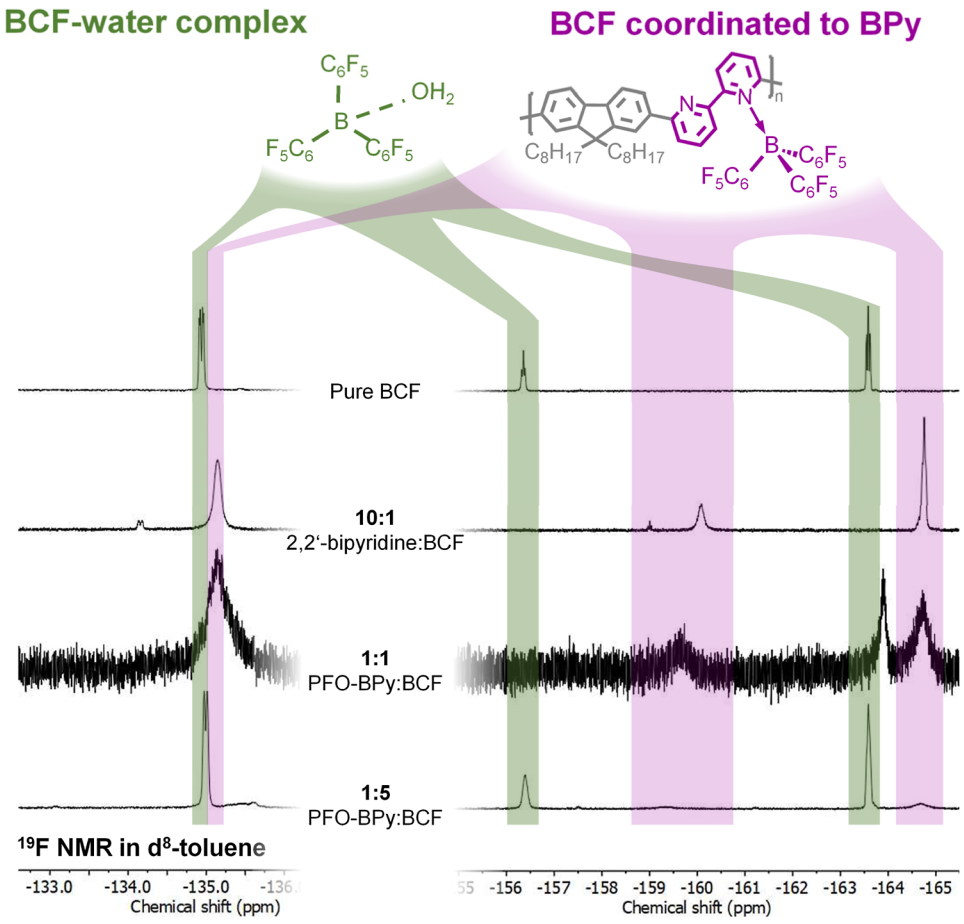

Figure 5. ^{19}F NMR spectra (546.73 MHz, d^8-toluene) of pure BCF, a 10:1 molar ratio of 2,2′-bipyridine/BCF, a 1:1 molar ratio PFO-BPy/BCF, and a 1:5 molar ratio of PFO-BPy/BCF (top to bottom). Green shaded areas indicate peaks associated with BCF:OH_2 complexes, and purple regions refer to peaks associated with BCF:BPy complexes. Schematic depictions of complexes are shown above the NMR spectra.

E_{11} absorption of (6,5) SWCNTs at around 990 nm in the absorption spectra (Figure 4a,b) and the radial breathing modes in the Raman spectra (Figure S1b). While usually undesired, these residual PFO-wrapped (6,5) SWCNTs enable a direct comparison to BCF-doping of the PFO-BPy-wrapped (6,5) SWCNTs.

Upon addition of up to 100 μg mL^{-1} of BCF to the dispersions, we observe similarly low bleaching of the (6,5) and (7,5) SWCNTs E_{11} absorption with or without additional PFO (see Figure 4a,b). For higher BCF concentrations, the (7,5) SWCNTs with 100 μg mL^{-1} PFO showed a stronger bleach than the (7,5) SWCNTs without added PFO. For the highest BCF concentration of 200 μg mL^{-1}, the trion absorption of the (7,5) SWCNTs at 1220 nm emerges. Overall, the bleaching remains below 60% and the E_{11} absorption peak remains well-defined with only a small blue-shift of 1 nm. In contrast to PFO-BPy (see inset in Figure 2a), PFO does not show any spectral signs of doping (see inset in Figure 4a) even for the highest BCF concentration of 200 μg mL^{-1}, which is consistent with the lack of doping of pure PFO solutions shown in Figure S5b,c as well as PFO film data by Zapata-Arteaga et al.[30]

The normalized bleaching values of the E_{11} absorption of (6,5) and (7,5) SWCNTs are shown in Figure 4c. While there is a stronger bleach of around 60% for the (7,5) SWCNTs at higher PFO concentrations (compared to ∼30% for the sample at lower PFO concentration), the differences for the PFO-wrapped (6,5) SWCNTs are negligible. Overall, these absorption spectra indicate only very limited doping of PFO-wrapped SWCNTs compared with PFO-BPy-wrapped SWCNTs under otherwise identical experimental conditions. Given the smaller bandgap of (7,5) SWCNTs compared to (6,5) SWCNTs, this experiment provides further evidence for a specific interaction of BCF with PFO-BPy and with PFO-BPy-wrapped SWCNTs.

BCF Doping Mechanism. The presented evidence for a synergistic interaction between BCF and PFO-BPy-wrapped nanotubes raises the question of a possible doping mechanism. Hence, we investigated the interaction and doping of pure PFO-BPy and PFO with BCF in more detail. Solutions of both polymers (100 μg mL^{-1} in toluene) were exposed to increasing amounts of BCF (see Figure S5a,b). While PFO showed no signs of bleaching or polaron formation, not even at much higher BCF/PFO ratios (50:1, Figure S5c), PFO-BPy was clearly p-doped as indicated by significant bleaching and red-shifted polaron absorption at BCF/PFO-BPy molar ratios above 1:1 (for calculation of molar ratios, see Methods). BCF only has an electron affinity of 4.81 eV (Figure 1a) and should not be able to dope any of the polymers via ICT or CTC. Previous studies also showed that PFO is not doped by the BCF:OH_2 complex.[30] Hence, the bipyridine unit of PFO-BPy must play a crucial role in doping the polymer.

To understand this behavior, we performed ^{19}F and ^{11}B NMR spectroscopy on solutions of PFO-BPy and the model

https://doi.org/10.1021/acs.jpcc.4c08584
J. Phys. Chem. C 2025, 129, 5520−5529

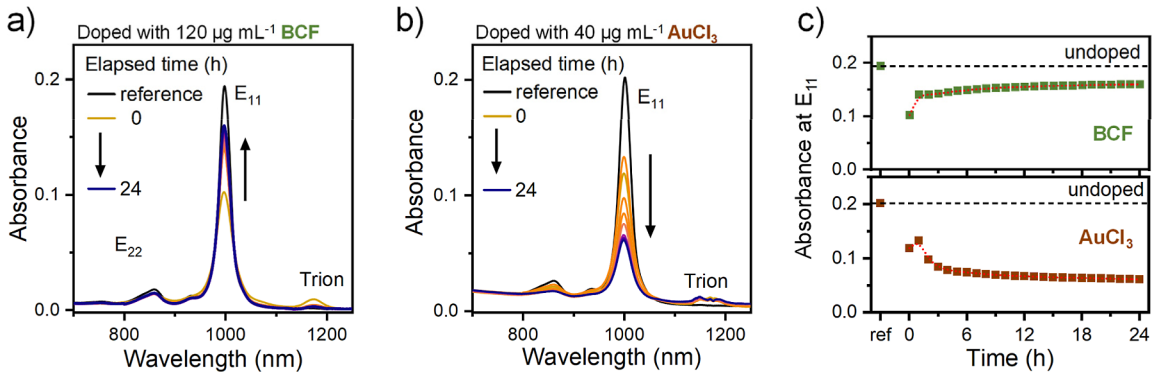

Figure 6. (a) Absorption spectra of (6,5) SWCNTs at a polymer concentration of 100 μg mL^{-1} doped with 120 μg mL^{-1} BCF over the course of 24 h. (b) Absorption spectra of (6,5) SWCNTs at a polymer concentration of 100 μg mL^{-1} doped with 40 μg mL^{-1} $AuCl_3$ over the course of 24 h. (c) E_{11} absorption of (6,5) SWCNTs doped with either BCF (top) or $AuCl_3$ (bottom) plotted against time after doping. The absorption of an undoped dispersion is indicated by a dashed line. The red dotted line serves as a guide to the eye.

compound 2,2′-bipyridine (BPy) in d^8-toluene that were doped with various amounts of BCF (Figures 5 and S10, S11). It is well-known that ^{11}B and ^{19}F NMR chemical shifts (δ) of organoboron compounds are especially sensitive to changes of the coordination state and ligand electronegativity. Trivalent organoboranes exhibit ^{11}B NMR shifts between 30 and 60 ppm, whereas tetravalent organoborates display significantly upfield-shifted ^{11}B NMR signals, typically in the range of −30 to 0 ppm.[52] In its pristine trivalent form BCF shows a single broad ^{11}B NMR peak at δ = 56 ppm,[53] as well as three ^{19}F NMR signals at δ = −129.5, −140.5, and −161.5 ppm.[54] When subjected to moisture (such as atmospheric humidity or trace amounts of water in solvents), BCF forms tetravalent complexes with water, as schematically shown in Figure 5. Hence, we only observe upfield-shifted ^{11}B NMR signals at δ = −1.6 ppm (Figure S10, top) and ^{19}F NMR signals at δ = −134.9, −156.4, and −163.6 ppm (Figure S11, top), confirming the presence of the tetravalent BCF:OH_2 complex.[53,54]

Since the only structural difference between the two wrapping polymers is a bipyridine unit, we used 2,2′-bipyridine (BPy) as a model compound to examine Lewis acid−base complexation in this system, as schematically shown in Figure 5. Providing a large excess of BPy (10:1 BPy/BCF) to achieve complete complexation of the BCF leads to a slight upfield shift of 1−4 ppm for the ^{19}F NMR signals and 2 ppm for the ^{11}B NMR signals. This is in agreement with previous reports of stronger shielding upon coordination of BCF to pyridinic nitrogen moieties and indicates a higher complexation strength compared to the BCF:OH_2 complex.[36]

For a 1:1 mixture of PFO-BPy/BCF (Figures 5 and S10, third trace), which does not yet show any signs of doping (Figure S5a), only the ^{19}F NMR and ^{11}B NMR signals of the complexed BCF are present. The small change in chemical shift of 0.5−1 ppm compared to the BCF:BPy complex can be explained by a slightly different chemical environment within the BCF:PFO-BPy complex. We also observe a significant line broadening compared to the BCF:OH_2 and BCF:BPy complex, which can be attributed to reduced molecular tumbling of the BCF molecules when complexed to the polymer.[55]

In contrast, the ^{19}F NMR spectrum of the 1:5 mixture of PFO-BPy/BCF (Figure 5, bottom trace) shows sharp peaks that can be assigned to the BCF:OH_2 complex. 10-fold magnification of the ^{19}F NMR spectrum (Figure S11), however, reveals that the broad signals of the BCF:PFO-BPy complex are still present. This is similar to the ^{11}B NMR spectrum, in which a sharp peak for the BCF:OH_2 complex and an underlying broad peak for the BCF:PFO-BPy complex is visible (Figure S10, bottom trace).

The NMR data together with the UV−vis absorption data strongly indicate that doping of PFO-BPy occurs via the Brønsted acidic BCF:OH_2 complex, which only forms after saturation of all polymer BPy units with BCF, and not via Lewis acid−base complexation. Despite having two possible coordination sites in a single BPy unit, one BCF molecule occupies both, as the addition of two mol equivalents of BCF already leads to substantial doping (Figure S5a). Applying these insights to the PFO-BPy-wrapped SWCNTs, we propose that the SWCNTs are not simply doped by BCF:OH_2 but through a unique interaction between BCF:OH_2 and the BCF:PFO-BPy complex. Such interaction also explains the dependence of the doping efficiency on the PFO-BPy concentration and the fact that significant doping occurred only above a 1:1 molar ratio of PFO-BPy/BCF for a PFO-BPy concentration of 100 μg mL^{-1}.

A possible doping mechanism for the SWCNTs might be inferred from previous work on the BCF-doping of polymers. For semiconducting polymers, Yurash et al. found a two-step doping mechanism with the first step being the protonation of a polymer chain by a BCF:OH_2 complex to create a positively charged chain segment and a $[BCF(OH)BCF]^-$ anion stabilized by a second BCF molecule.[38] The doping process is completed by intra- or interchain electron transfer from a neutral chain segment to the protonation site.[37,38] For the PFO-BPy-wrapped SWCNTs, we propose a similar three-step mechanism: (1) Lewis acid−base complexation of BCF by the PFO-BPy bipyridine units up to a 1:1 molar ratio. (2) Protonation of the PFO-BPy wrapped around the SWCNTs by BCF:OH_2 and formation of a $[BCF(OH)BCF]^-$ anion. (3) Electron transfer from the SWCNT (instead of a neutral polymer chain segment) to the doped PFO-BPy polymer segments leading to p-doping of the SWCNT. The proposed steps are visualized in Figure S12. Note that this process would not be possible with PFO-wrapped SWCNTs because the polymer would not be doped without the presence of the bipyridine units and the resulting BCF complex. Although this mechanism is consistent with the available experimental data, further theoretical studies are needed to resolve the details.

BCF versus Other Common p-Dopants. Regardless of the precise doping mechanism, one of the main questions is

https://doi.org/10.1021/acs.jpcc.4c08584
J. Phys. Chem. C 2025, 129, 5520−5529

whether BCF-doping provides any advantages compared with other common molecular dopants for SWCNTs. Various oxidants have been applied to obtain p-doped (6,5) or other SWCNTs.[48,50,56] Due to their large bandgap, (6,5) SWCNTs usually require fairly strong p-dopants compared to larger diameter nanotubes. Typical dopants include F_4TCNQ but also $AuCl_3$. F_4TCNQ suffers from several disadvantages as a p-dopant for polymer-wrapped small-diameter SWCNTs. It is barely soluble in nonpolar solvents such as toluene, while BCF is highly soluble. Despite an EA of 5.26 eV, F_4TCNQ is not able to induce strong doping in small diameter nanotubes as shown in Figure 3. The maximum E_{11} bleach values are below 40%. Furthermore, the intense absorption of F_4TCNQ and F_4TCNQ anions[56] between 400 and 700 nm makes analysis of any changes in E_{22} or PFO-BPy absorption impossible. In contrast to that, BCF does not have any absorption bands in the visible range.[29]

$AuCl_3$ is a very strong dopant that is often used for spectroscopic studies of small-diameter SWCNTs.[47,48,50] Only low concentrations of $AuCl_3$ are required for efficient doping, and it has no absorption features that would obstruct spectral analysis. However, $AuCl_3$ is essentially insoluble in nonpolar solvents such as toluene. Hence, a mixture of acetonitrile and toluene is usually used for doping in a dispersion, which reduces the dispersion stability significantly.

The difference in long-term stability between doping of (6,5) SWCNTs with BCF and $AuCl_3$ is demonstrated in Figure 6. A (6,5) SWCNT dispersion with 100 μg mL^{-1} PFO-BPy in a 1:5 mixture of acetonitrile/toluene was doped with 40 μg mL^{-1} $AuCl_3$ and compared to a similar dispersion with only toluene as the solvent doped with 120 μg mL^{-1} of BCF. Doping with BCF results in an initial absorption bleach of E_{11} of around 50%. The absorption increases again within the first hour and then stabilizes at around 75−80% of the initial absorption value (Figure 6a,c). The PFO-BPy polaron absorption is decreasing simultaneously (see Figure S13), which points toward slight dedoping of the polymer and the SWCNTs. The same dedoping behavior can be observed for a BCF concentration of 200 μg mL^{-1}, which led to higher initial doping level of the (6,5) SWCNT (Figure S14). In this case, the E_{11} absorption stabilizes after 6 h at 25% of the original absorption. These observations indicate a loss of BCF possibly due to side reactions, e.g., with residual water. While this means that samples should be measured instantly to correlate doping concentration with doping level, the intrinsic dedoping over time also provides an opportunity to measure the same sample at various doping levels without additional sample preparation. Importantly, there are no signs of aggregation (Figure S15), which makes BCF an interesting dopant for spectroscopic studies of doped (6,5) SWCNTs in dispersion.

In contrast to that, the (6,5) SWCNT dispersion in toluene/acetonitrile shows an increased scattering background (see Figure 6b), indicating SWCNT aggregation despite previous sonication. Upon addition of $AuCl_3$, the E_{11} absorption is bleached to ∼60% of its initial value. Within the first hour, $AuCl_3$ the E_{11} absorption starts to increase again, indicating dedoping but then decreases (Figure 6c). This loss of absorption is due to strong nanotube aggregation[57] not increased doping as the corresponding absorption spectra do not show higher trion absorption but the scattering background increases. Indeed, visual inspection of the cuvette reveals clouds of aggregated SWCNTs for $AuCl_3$ doping (Figure S15). This renders $AuCl_3$ a less-than-ideal dopant for extended doping experiments on SWCNTs and shows the potential of BCF as a dopant for detailed spectroscopic studies of SWCNT dispersions.

CONCLUSIONS

In this study, we explored the unique p-doping of PFO-BPy-wrapped (6,5) SWCNTs by BCF. Despite its comparatively low electron affinity, BCF is able to induce efficient p-doping of small-diameter PFO-BPy-wrapped (6,5) SWCNTs, while it does not dope PFO-wrapped (7,5) SWCNTs. The increase of BCF doping strength with higher PFO-BPy concentrations, an effect that is not observed for other dopants such as F_4TCNQ, as well as the simultaneous doping of the PFO-BPy and the (6,5) SWCNTs indicate a specific interaction between BCF, the bipyridine groups of the PFO-BPy and the nanotubes. Based on the proposed BCF-doping mechanism for semiconducting polymers, we suggest a three-step process that involves the complexation of BCF by the bipyridine of the polymer, protonation of the PFO-BPy that is wrapped around the SWCNTs by BCF:OH_2 and formation of a $[BCF(OH)\text{-}BCF]^-$ anion, and finally electron transfer from the SWCNT to the protonated PFO-BPy polymer. The applicability of BCF as an efficient dopant should not be limited to PFO-BPy-wrapped SWCNTs as there are several conjugated polymers, which are applied for nanotube sorting and contain Lewis-basic nitrogen.[58,59] Overall, BCF is an excellent dopant for small-diameter, polymer-wrapped SWCNTs in toluene dispersions with a higher doping efficiency than F_4TCNQ and much better long-term dispersion stability than doping with $AuCl_3$. These properties are especially important for fundamental spectroscopic studies of the interactions of charge carriers with excitons in one-dimensional nanotubes without any spectral broadening or energy transfer, which are usually observed for aggregates, networks, or dense films.

ASSOCIATED CONTENT

Supporting Information

The Supporting Information is available free of charge at https://pubs.acs.org/doi/10.1021/acs.jpcc.4c08584.

Raman and absorption spectra of undoped polymer-wrapped (6,5) and (7,5) SWCNTs, ^{11}B and ^{19}F NMR and absorption spectra of BCF-doped wrapping polymers, additional data on BCF doping of polymer-wrapped SWCNTs (absorption spectra of additional BCF concentrations, analysis of E_{11}, polaron and trion bands as a function of BCF concentration, analysis of PFO-BPy polaron position for BCF doping), schematic illustration of the proposed doping mechanism, and photographs of SWCNT dispersions doped with $AuCl_3$ or BCF after 24 h (PDF)

AUTHOR INFORMATION

Corresponding Author

Jana Zaumseil − *Institute for Physical Chemistry, Heidelberg University, D-69120 Heidelberg, Germany;* orcid.org/0000-0002-2048-217X; Email: zaumseil@uni-heidelberg.de

Authors

Sebastian Lindenthal − *Institute for Physical Chemistry, Heidelberg University, D-69120 Heidelberg, Germany*

https://doi.org/10.1021/acs.jpcc.4c08584
J. Phys. Chem. C 2025, 129, 5520−5529

Daniel Rippel − *Institute for Physical Chemistry, Heidelberg University, D-69120 Heidelberg, Germany*
Lucas Kistner − *Institute for Inorganic Chemistry, Heidelberg University, D-69120 Heidelberg, Germany*
Angus Hawkey − *Institute for Physical Chemistry, Heidelberg University, D-69120 Heidelberg, Germany*

Complete contact information is available at: https://pubs.acs.org/10.1021/acs.jpcc.4c08584

Author Contributions

S.L. processed and measured all samples and analyzed the data with help from D.R. and A.H. L.K. assisted in measuring and analyzing NMR data. J.Z. conceived and supervised the project. S.L. and J.Z. wrote the manuscript with input from all authors. All authors have given approval to the final version of the manuscript.

Notes

The authors declare no competing financial interest.

■ ACKNOWLEDGMENTS

The authors acknowledge financial support by the Deutsche Forschungsgemeinschaft (DFG, German Research Foundation) via SFB 1225/3 (Isoquant). A.H. received funding from the European Union's Horizon 2020 research and innovation program under the Marie Skłodowska-Curie grant agreement no. 955837 (HORATES). The authors also thank Prof. H.-J. Himmel and J. Doll for assistance with NMR measurements.

■ REFERENCES

(1) Charlier, J. C.; Blase, X.; Roche, S. Electronic and transport properties of nanotubes. *Rev. Mod. Phys.* **2007**, *79*, 677−732.
(2) Weisman, R. B.; Bachilo, S. M. Dependence of Optical Transition Energies on Structure for Single-Walled Carbon Nanotubes in Aqueous Suspension: An Empirical Kataura Plot. *Nano Lett.* **2003**, *3*, 1235−1238.
(3) Nish, A.; Hwang, J.-Y.; Doig, J.; Nicholas, R. J. Highly selective dispersion of single-walled carbon nanotubes using aromatic polymers. *Nat. Nanotechnol.* **2007**, *2*, 640−646.
(4) Mistry, K. S.; Larsen, B. A.; Blackburn, J. L. High-Yield Dispersions of Large-Diameter Semiconducting Single-Walled Carbon Nanotubes with Tunable Narrow Chirality Distributions. *ACS Nano* **2013**, *7*, 2231−2239.
(5) Salazar-Rios, J. M.; Talsma, W.; Derenskyi, V.; Gomulya, W.; Keller, T.; Fritsch, M.; Kowalski, S.; Preis, E.; Wang, M.; Allard, S.; Bazan, G. C.; Scherf, U.; dos Santos, M. C.; Loi, M. A. Understanding the Selection Mechanism of the Polymer Wrapping Technique toward Semiconducting Carbon Nanotubes. *Small Methods* **2018**, *2*, 1700335.
(6) Gao, J.; Loi, M. A.; de Carvalho, E. J. F.; dos Santos, M. C. Selective Wrapping and Supramolecular Structures of Polyfluorene−Carbon Nanotube Hybrids. *ACS Nano* **2011**, *5*, 3993−3999.
(7) Kahmann, S.; Salazar Rios, J. M.; Zink, M.; Allard, S.; Scherf, U.; dos Santos, M. C.; Brabec, C. J.; Loi, M. A. Excited-State Interaction of Semiconducting Single-Walled Carbon Nanotubes with Their Wrapping Polymers. *J. Phys. Chem. Lett.* **2017**, *8*, 5666−5672.
(8) Balcı Leinen, M.; Berger, F. J.; Klein, P.; Mühlinghaus, M.; Zorn, N. F.; Settele, S.; Allard, S.; Scherf, U.; Zaumseil, J. Doping-Dependent Energy Transfer from Conjugated Polyelectrolytes to (6,5) Single-Walled Carbon Nanotubes. *J. Phys. Chem. C* **2019**, *123*, 22680−22689.
(9) Guo, C.; Ouyang, J.; Shin, H.; Ding, J.; Li, Z.; Lapointe, F.; Lefebvre, J.; Kell, A. J.; Malenfant, P. R. L. Enrichment of Semiconducting Single-Walled Carbon Nanotubes with Indigo-Fluorene-Based Copolymers and Their Use in Printed Thin-Film Transistors and Carbon Dioxide Gas Sensors. *ACS Sens.* **2020**, *5*, 2136−2145.
(10) Ozawa, H.; Ide, N.; Fujigaya, T.; Niidome, Y.; Nakashima, N. One-pot Separation of Highly Enriched (6,5)-Single-walled Carbon Nanotubes Using a Fluorene-based Copolymer. *Chem. Lett.* **2011**, *40*, 239−241.
(11) Zhao, W.; Ding, J.; Zou, Y.; Di, C.-a.; Zhu, D. Chemical doping of organic semiconductors for thermoelectric applications. *Chem. Soc. Rev.* **2020**, *49*, 7210−7228.
(12) Blackburn, J. L.; Ferguson, A. J.; Cho, C.; Grunlan, J. C. Carbon-Nanotube-Based Thermoelectric Materials and Devices. *Adv. Mater.* **2018**, *30*, 1704386.
(13) Hofmann, A. I.; Kroon, R.; Zokaei, S.; Järsvall, E.; Malacrida, C.; Ludwigs, S.; Biskup, T.; Müller, C. Chemical Doping of Conjugated Polymers with the Strong Oxidant Magic Blue. *Adv. Electron. Mater.* **2020**, *6*, 2000249.
(14) Matsunaga, R.; Matsuda, K.; Kanemitsu, Y. Observation of Charged Excitons in Hole-Doped Carbon Nanotubes Using Photoluminescence and Absorption Spectroscopy. *Phys. Rev. Lett.* **2011**, *106*, 037404.
(15) Eckstein, K. H.; Hartleb, H.; Achsnich, M. M.; Schöppler, F.; Hertel, T. Localized Charges Control Exciton Energetics and Energy Dissipation in Doped Carbon Nanotubes. *ACS Nano* **2017**, *11*, 10401−10408.
(16) Salzmann, I.; Heimel, G.; Oehzelt, M.; Winkler, S.; Koch, N. Molecular Electrical Doping of Organic Semiconductors: Fundamental Mechanisms and Emerging Dopant Design Rules. *Acc. Chem. Res.* **2016**, *49*, 370−378.
(17) Lüssem, B.; Keum, C.-M.; Kasemann, D.; Naab, B.; Bao, Z.; Leo, K. Doped Organic Transistors. *Chem. Rev.* **2016**, *116*, 13714−13751.
(18) Jacobs, I. E.; Moulé, A. J. Controlling Molecular Doping in Organic Semiconductors. *Adv. Mater.* **2017**, *29*, 1703063.
(19) Arias, A. C.; MacKenzie, J. D.; McCulloch, I.; Rivnay, J.; Salleo, A. Materials and Applications for Large Area Electronics: Solution-Based Approaches. *Chem. Rev.* **2010**, *110*, 3−24.
(20) Li, J.; Zhang, G.; Holm, D. M.; Jacobs, I. E.; Yin, B.; Stroeve, P.; Mascal, M.; Moulé, A. J. Introducing Solubility Control for Improved Organic P-Type Dopants. *Chem. Mater.* **2015**, *27*, 5765−5774.
(21) Kumar, J.; Singh, R. K.; Singh, R.; Rastogi, R. C.; Kumar, V. Effect of FeCl3 on the stability of π-conjugation of electronic polymer. *Corros. Sci.* **2008**, *50*, 301−308.
(22) Jha, M.; Mogollon Santiana, J.; Jacob, A. A.; Light, K.; Hong, M. L.; Lau, M. R.; Filardi, L. R.; Miao, H.; Gurses, S. M.; Kronawitter, C. X.; Mascal, M.; Moulé, A. J. Stability Study of Molecularly Doped Semiconducting Polymers. *J. Phys. Chem. C* **2024**, *128*, 1258−1266.
(23) Han, C. C.; Elsenbaumer, R. L. Protonic acids: Generally applicable dopants for conducting polymers. *Synth. Met.* **1989**, *30*, 123−131.
(24) Polk, B. J.; Potje-Kamloth, K.; Josowicz, M.; Janata, J. Role of Protonic and Charge Transfer Doping in Solid-State Polyaniline. *J. Phys. Chem. B* **2002**, *106*, 11457−11462.
(25) Strano, M. S.; Huffman, C. B.; Moore, V. C.; O'Connell, M. J.; Haroz, E. H.; Hubbard, J.; Miller, M.; Rialon, K.; Kittrell, C.; Ramesh, S.; Hauge, R. H.; Smalley, R. E. Reversible, Band-Gap-Selective Protonation of Single-Walled Carbon Nanotubes in Solution. *J. Phys. Chem. B* **2003**, *107*, 6979−6985.
(26) Kim, S. M.; Jo, Y. W.; Kim, K. K.; Duong, D. L.; Shin, H.-J.; Han, J. H.; Choi, J.-Y.; Kong, J.; Lee, Y. H. Transparent Organic P-Dopant in Carbon Nanotubes: Bis(trifluoromethanesulfonyl)imide. *ACS Nano* **2010**, *4*, 6998−7004.
(27) Ausserlechner, S. J.; Gruber, M.; Hetzel, R.; Flesch, H.-G.; Ladinig, L.; Hauser, L.; Haase, A.; Buchner, M.; Resel, R.; Schürrer, F.; Stadlober, B.; Trimmel, G.; Zojer, K.; Zojer, E. Mechanism of surface proton transfer doping in pentacene based organic thin-film transistors. *Phys. Status Solidi A* **2012**, *209*, 181−192.
(28) Bridges, C. R.; Baumgartner, T. Lewis acids and bases as molecular dopants for organic semiconductors. *J. Phys. Org. Chem.* **2020**, *33*, No. e4077.

(29) Welch, G. C.; Coffin, R.; Peet, J.; Bazan, G. C. Band Gap Control in Conjugated Oligomers via Lewis Acids. *J. Am. Chem. Soc.* **2009**, *131*, 10802−10803.
(30) Zapata-Arteaga, O.; Perevedentsev, A.; Prete, M.; Busato, S.; Floris, P. S.; Asatryan, J.; Rurali, R.; Martín, J.; Campoy-Quiles, M. A Universal, Highly Stable Dopant System for Organic Semiconductors Based on Lewis-Paired Dopant Complexes. *ACS Energy Lett.* **2024**, *9*, 3567−3577.
(31) Zalar, P.; Henson, Z. B.; Welch, G. C.; Bazan, G. C.; Nguyen, T.-Q. Color Tuning in Polymer Light-Emitting Diodes with Lewis Acids. *Angew. Chem., Int. Ed.* **2012**, *51*, 7495−7498.
(32) Zalar, P.; Kuik, M.; Henson, Z. B.; Woellner, C.; Zhang, Y.; Sharenko, A.; Bazan, G. C.; Nguyen, T.-Q. Increased Mobility Induced by Addition of a Lewis Acid to a Lewis Basic Conjugated Polymer. *Adv. Mater.* **2014**, *26*, 724−727.
(33) Han, Y.; Barnes, G.; Lin, Y.-H.; Martin, J.; Al-Hashimi, M.; AlQaradawi, S. Y.; Anthopoulos, T. D.; Heeney, M. Doping of Large Ionization Potential Indenopyrazine Polymers via Lewis Acid Complexation with Tris(pentafluorophenyl)borane: A Simple Method for Improving the Performance of Organic Thin-Film Transistors. *Chem. Mater.* **2016**, *28*, 8016−8024.
(34) Yan, H.; Chen, J.; Zhou, K.; Tang, Y.; Meng, X.; Xu, X.; Ma, W. Lewis Acid Doping Induced Synergistic Effects on Electronic and Morphological Structure for Donor and Acceptor in Polymer Solar Cells. *Adv. Energy Mater.* **2018**, *8*, 1703672.
(35) Yan, H.; Tang, Y.; Sui, X.; Liu, Y.; Gao, B.; Liu, X.; Liu, S. F.; Hou, J.; Ma, W. Increasing Quantum Efficiency of Polymer Solar Cells with Efficient Exciton Splitting and Long Carrier Lifetime by Molecular Doping at Heterojunctions. *ACS Energy Lett.* **2019**, *4*, 1356−1363.
(36) Suh, E. H.; Kim, S. B.; Yang, H. S.; Jang, J. Regulating Competitive Doping in Solution-Mixed Conjugated Polymers for Dramatically Improving Thermoelectric Properties. *Adv. Funct. Mater.* **2022**, *32*, 2207413.
(37) Yurash, B.; Cao, D. X.; Brus, V. V.; Leifert, D.; Wang, M.; Dixon, A.; Seifrid, M.; Mansour, A. E.; Lungwitz, D.; Liu, T.; Santiago, P. J.; Graham, K. R.; Koch, N.; Bazan, G. C.; Nguyen, T.-Q. Towards understanding the doping mechanism of organic semiconductors by Lewis acids. *Nat. Mater.* **2019**, *18*, 1327−1334.
(38) Marqués, P. S.; Londi, G.; Yurash, B.; Nguyen, T.-Q.; Barlow, S.; Marder, S. R.; Beljonne, D. Understanding how Lewis acids dope organic semiconductors: a "complex" story. *Chem. Sci.* **2021**, *12*, 7012−7022.
(39) Vijayakumar, V.; Durand, P.; Zeng, H.; Untilova, V.; Herrmann, L.; Algayer, P.; Leclerc, N.; Brinkmann, M. Influence of dopant size and doping method on the structure and thermoelectric properties of PBTTT films doped with F6TCNNQ and F4TCNQ. *J. Mater. Chem. C* **2020**, *8*, 16470−16482.
(40) Lu, H.; Guo, Y.; Robertson, J. Charge transfer doping of graphene without degrading carrier mobility. *J. Appl. Phys.* **2017**, *121*, 224304.
(41) Tanaka, Y.; Hirana, Y.; Niidome, Y.; Kato, K.; Saito, S.; Nakashima, N. Experimentally Determined Redox Potentials of Individual (n,m) Single-Walled Carbon Nanotubes. *Angew. Chem., Int. Ed.* **2009**, *48*, 7655−7659.
(42) Park, K. H.; Lee, S.-H.; Toshimitsu, F.; Lee, J.; Park, S. H.; Tsuyohiko, F.; Jang, J.-W. Gate-enhanced photocurrent of (6,5) single-walled carbon nanotube based field effect transistor. *Carbon* **2018**, *139*, 709−715.
(43) Graf, A.; Zakharko, Y.; Schießl, S. P.; Backes, C.; Pfohl, M.; Flavel, B. S.; Zaumseil, J. Large scale, selective dispersion of long single-walled carbon nanotubes with high photoluminescence quantum yield by shear force mixing. *Carbon* **2016**, *105*, 593−599.
(44) Lindenthal, S.; Settele, S.; Hellmann, J.; Schmitt, K.; Zaumseil, J. A Hands-On Guide to Shear Force Mixing of Single-Walled Carbon Nanotubes with Conjugated Polymers. *arXiv* **2023**, arXiv:2311.11654v1.
(45) Pfohl, M.; Tune, D. D.; Graf, A.; Zaumseil, J.; Krupke, R.; Flavel, B. S. Fitting Single-Walled Carbon Nanotube Optical Spectra. *ACS Omega* **2017**, *2*, 1163−1171.
(46) Shea, M. J.; Mehlenbacher, R. D.; Zanni, M. T.; Arnold, M. S. Experimental Measurement of the Binding Configuration and Coverage of Chirality-Sorting Polyfluorenes on Carbon Nanotubes. *J. Phys. Chem. Lett.* **2014**, *5*, 3742−3749.
(47) Eckstein, K. H.; Oberndorfer, F.; Achsnich, M. M.; Schöppler, F.; Hertel, T. Quantifying Doping Levels in Carbon Nanotubes by Optical Spectroscopy. *J. Phys. Chem. C* **2019**, *123*, 30001−30006.
(48) Hawkey, A.; Dash, A.; Rodríguez-Martínez, X.; Zhao, Z.; Champ, A.; Lindenthal, S.; Zharnikov, M.; Kemerink, M.; Zaumseil, J. Ion-Exchange Doping of Semiconducting Single-Walled Carbon Nanotubes. *Adv. Mater.* **2024**, *36*, 2404554.
(49) Liu, Y.; Zhao, Z.; Kang, L.; Qiu, S.; Li, Q. Molecular Doping Modulation and Applications of Structure-Sorted Single-Walled Carbon Nanotubes: A Review. *Small* **2024**, *20*, 2304075.
(50) Eckstein, K. H.; Kunkel, P.; Voelckel, M.; Schöppler, F.; Hertel, T. Trions, Exciton Dynamics, and Spectral Modifications in Doped Carbon Nanotubes: A Singular Defect-Driven Mechanism. *J. Phys. Chem. C* **2023**, *127*, 19659−19667.
(51) Hartmann, N. F.; Pramanik, R.; Dowgiallo, A.-M.; Ihly, R.; Blackburn, J. L.; Doorn, S. K. Photoluminescence Imaging of Polyfluorene Surface Structures on Semiconducting Carbon Nanotubes: Implications for Thin Film Exciton Transport. *ACS Nano* **2016**, *10*, 11449−11458.
(52) Wrackmeyer, B. Organoboranes and tetraorganoborates studied by 11B and 13C NMR spectroscopy and DFT calculations. *Z. Naturforsch., B* **2015**, *70*, 421−424.
(53) Yurash, B.; Leifert, D.; Reddy, G. N. M.; Cao, D. X.; Biberger, S.; Brus, V. V.; Seifrid, M.; Santiago, P. J.; Köhler, A.; Chmelka, B. F.; Bazan, G. C.; Nguyen, T.-Q. Atomic-Level Insight into the Postsynthesis Band Gap Engineering of a Lewis Base Polymer Using Lewis Acid Tris(pentafluorophenyl)borane. *Chem. Mater.* **2019**, *31*, 6715−6725.
(54) Beringhelli, T.; Maggioni, D.; D'Alfonso, G. 1H and 19F NMR Investigation of the Reaction of B(C6F5)3 with Water in Toluene Solution. *Organometallics* **2001**, *20*, 4927−4938.
(55) Bovey, F. A. The high resolution NMR spectroscopy of polymers. *Prog. Polym. Sci.* **1971**, *3*, 1−108.
(56) Stanton, N. J.; Ihly, R.; Norton-Baker, B.; Ferguson, A. J.; Blackburn, J. L. Solution-phase p-type doping of highly enriched semiconducting single-walled carbon nanotubes for thermoelectric thin films. *Appl. Phys. Lett.* **2021**, *119*, 023302.
(57) Schneider, S.; Lefebvre, J.; Diercks, N. J.; Berger, F. J.; Lapointe, F.; Schleicher, J.; Malenfant, P. R. L.; Zaumseil, J. Phenanthroline Additives for Enhanced Semiconducting Carbon Nanotube Dispersion Stability and Transistor Performance. *ACS Appl. Nano Mater.* **2020**, *3*, 12314−12324.
(58) Berton, N.; Lemasson, F.; Poschlad, A.; Meded, V.; Tristram, F.; Wenzel, W.; Hennrich, F.; Kappes, M. M.; Mayor, M. Selective Dispersion of Large-Diameter Semiconducting Single-Walled Carbon Nanotubes with Pyridine-Containing Copolymers. *Small* **2014**, *10*, 360−367.
(59) Gu, J.; Han, J.; Liu, D.; Yu, X.; Kang, L.; Qiu, S.; Jin, H.; Li, H.; Li, Q.; Zhang, J. Solution-Processable High-Purity Semiconducting SWCNTs for Large-Area Fabrication of High-Performance Thin-Film Transistors. *Small* **2016**, *12*, 4993−4999.

https://doi.org/10.1021/acs.jpcc.4c08584
J. Phys. Chem. C 2025, 129, 5520−5529